3D Structured Optical Fiber Pressure Sensors Based on Femtosecond Laser Fabrication

Tongyu Liu,[1,3] Zipei Song,[1] Mohan Wang,[1] Crispin T.M. Doyle,[2] Martin J. Booth[1] and Julian A.J. Fells[1,4]

[1] *Department of Engineering Science, University of Oxford, Parks Road, Oxford OX1 3PJ, UK*
[2] *Halliburton, Spectrum House, Brants Bridge, Bracknell RG12 9BG, UK*

[3] *tongyu.liu@stcatz.ox.ac.uk*
[4] *julian.fells@eng.ox.ac.uk*

Abstract: Pressure sensors based on air-hole fiber have limitations in design and materials. We fabricate and test pressure sensors with complex 3D structures in commercial fibers, with potential for many types of high-performance fibers.
© 2023 The Author(s)

1. Introduction

Pressure sensors are needed for monitoring a wide range of infrastructure for performance and safety. Compared to traditional electronic sensors, the optical fiber sensors are immune to electromagnetic interference and able to operate in explosive environments [1]. Many applications, such as space and aerospace are very sensitive to mass and size, and optical fiber sensors have very significant advantages over traditional electronic sensors in this respect [2]. Furthermore, there is a desire to extend pressure monitoring into ultra-extreme environments such as gas turbines and nuclear reactors, beyond the capabilities of silica fiber.

Fabry-Perot sensors have been used for pressure sensing, but these are unsuitable for multiplexing multiple sensors on a single fiber [3]. An alternative solution is to use optical fiber drawn with air holes in the cladding all the way along the length of the fiber [4, 5]. When exposed to external pressure, there is a stress induced birefringence, which can be detected with polarimetry. Fiber Bragg gratings (FBGs) may be incorporated into this fiber for high sensitivity pressure measurements at specific points. These sensors have two Bragg reflection peaks and their wavelength separation is a measure of pressure, while their absolute wavelengths can be used to determine temperature [4, 6]. The sensitivity has been further improved using a microstructure air hole fiber [7]. However, there is a mode mismatch between these speciality fibers and standard single mode fiber, resulting in high splice losses, which can severely restrict the number of concatenated sensors. For example, the round trip splice loss in Ref. [7] was 12 dB. In this paper, we design and fabricate three-dimensional custom holes in step-index fiber to allow high sensitivity without incurring large splice losses. The technique also has the potential for use in exotic fibers for ultra-extreme environments.

2. Sensor design

Incorporating air holes into an optical fiber will result in an uneven stress distribution inside the fiber when subjected to external pressure. This in turn will cause the refractive index of the fiber to become anisotropic via the stress-optic effect [8]. The relation between the stress and the induced refractive index change can be described by,

$$\begin{aligned} n_1 &= n_0 - 0.5n_0^3(P_{11}\varepsilon_x + P_{12}\varepsilon_y + P_{12}\varepsilon_z) \\ n_2 &= n_0 - 0.5n_0^3(P_{12}\varepsilon_x + P_{11}\varepsilon_y + P_{12}\varepsilon_z) \\ n_3 &= n_0 - 0.5n_0^3(P_{12}\varepsilon_x + P_{12}\varepsilon_y + P_{11}\varepsilon_z) \end{aligned} \tag{1}$$

where P_{11}, P_{12} are the stress-optic coefficients, ε_x,ε_y,ε_z are the stress components, n_1, n_2, n_3 are the refractive index components and n_0 is the unstressed refractive index. This anisotropy will change the effective refractive index of the fiber in the two orthogonal polarization modes. According to the Bragg equation, the central reflection wavelength of the FBG will shift as the effective refractive index changes. Hence, since the orthogonal polarization modes have different effective indices, they will also have different Bragg wavelengths. This will result in a splitting of the reflection peak if light is launched into both polarizations. In contrast, although the refractive index will also change with temperature, this change is isotropic and will not cause the reflection peak to split.

To model and optimise the structure of the sensor, We used the multi-physics field simulation software COMSOL to calculate the distribution of internal stresses in the fiber when it is exposed to external pressure. Then we calculated the refractive index distribution by bringing the results of the stress distribution into the stress-optic equation. We simulate the FBG in the modified fiber based on these data and calculate its transmission peak. We then get the response of the sensor under external pressure changes. We investigated sensors in both standard single-mode fiber (SMF) and a large cladding fiber (LCF) with 250 μm diameter (LIEKKI Passive-20/250DC). This fiber was few-moded at 1550 nm, but single moded above 1640 nm.

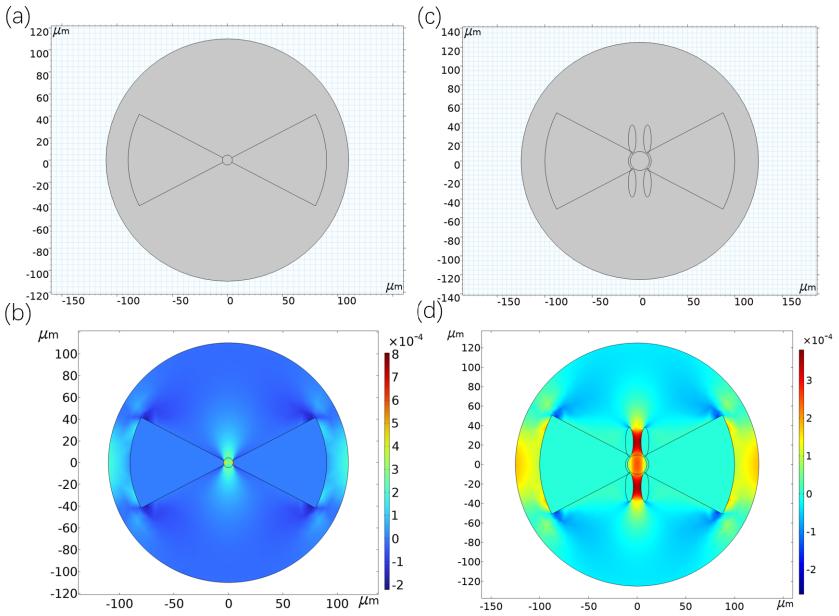


Fig. 1. Simulation results of the distribution of the change in refractive index components over different fiber cross-sections when an external 124 bar pressure is applied. (a), (c) Schematic diagram of the sector holes and the sector holes with elliptical micro-holes. (b), (d) Simulation results for the distribution of the change in refractive index components.

The starting point for the design is like a bow-tie, consisting of two sectors filled with air. Figure 1 shows the simulation results. Different shapes and sizes of air holes can have a significant effect on the sensitivity of the sensor. Adding multiple micro-holes around the fiber core can improve sensitivity considerably. In addition, we also experimented with changing some other shape parameters to explore their effect on sensitivity such as the sector angle. We set the radius of the sector to 90 μm and performed a parameter sweep for the sector angle, which ranged from 40° to 90°. If the angle is too large the hollow area will also become too large and the sensor structure will be unstable. The results in Figure 3(a) show the maximum transmission peak separation is 0.3 nm for a sector angle of 55 degrees at an external pressure of 124 bar.

Diameter	Type	Sensitivity
125 μm	Sector hole	1.128 pm/bar
220 μm	Sector hole	2.417 pm/bar
250 μm	Sector hole with elliptical micro-holes	3.304 pm/bar

Fig. 2. Simulation results of sensitivity in different types of optical fiber.

After analysing the influence of the shape of the air holes, it is also critical to ensure that temperature changes can be decoupled from pressure changes. We introduced thermal expansion into the model to calculate the transmission spectra at different pressures and temperatures and obtained the simulation results as shown in Figure 3(b). It is clear that at different temperatures, the relative distance between the two orthogonal mode peaks changes slightly and is more just an overall translation. However, the distances of peak separation change stably at different pressures. This also means that temperature and pressure data can be acquired simultaneously for this type

of sensor. Finally, simulation of the transmission spectrum of the same sensor at different pressures leads to the results in Fig. 3(c), where the pressure shows a linear relationship with the peak separation.

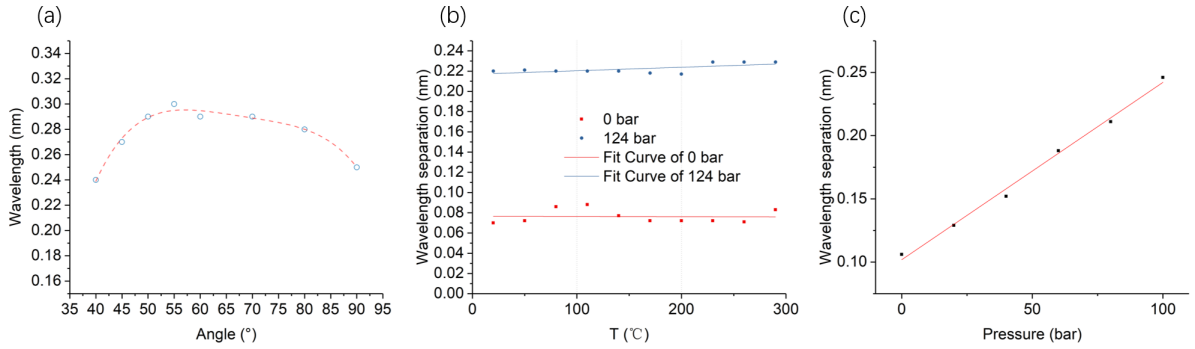


Fig. 3. (a) Parameter sweep for the sector angle. (b) Simulation results of peak separation at different temperatures and pressures. (c) Relation between wavelength separation and pressure change.

3. Fabrication and testing

The devices were fabricated by first exposing the fiber to a femtosecond laser to define the areas to be removed. The fibers were then placed in an etchant to selectively remove these defined areas. The laser used for sample fabrication was a femtosecond laser (Light Conversion, Pharos) operating at 515 nm with a linear polarization and an oil immersion objective (Olympus UPlanAPO 20x, NA0.85). The laser power used were in the range of 90 mW to 130 mW. Sensors with sector air-holes were fabricated in the SMF and sensors with sectors and elliptical micro-holes were fabricated in the LCF.

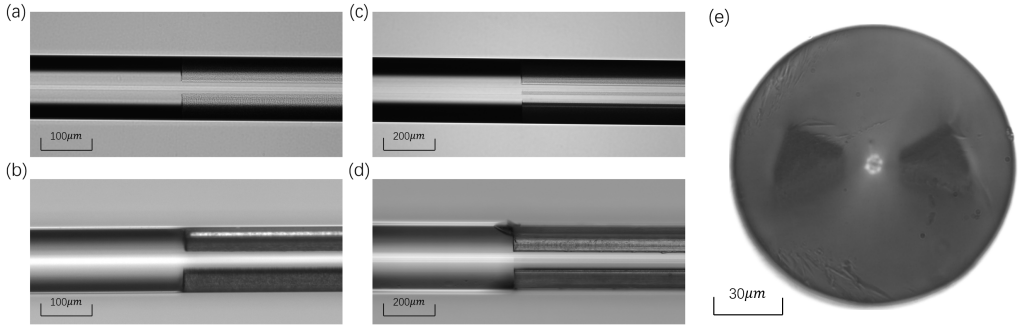


Fig. 4. Microscope image of the samples. (a),(b) Side views of the inscribed and uninscribed areas of the 125 μm SMF before and after etching. (c),(d) Side views of the inscribed and uninscribed areas of the 250 μm few modes fiber before and after etching. (e) Cross-sectional view of the 125 μm SMF inscription area.

We used 8 mol/L KOH at 85°C for wet etching of the silica fiber because KOH has better selectivity than HF and it is also less hazardous [9, 10]. The micrograph in Fig. 4 demonstrates the accuracy of this selective etching. Although the etched area appears to be through the fiber cladding, this is an illusion caused by aberrations.

A LCF sample (80 μm sector holes with micro-holes) smaller than the simulated model (100 μm sector holes with micro-holes) was pressure tested at Halliburton. The samples were spliced to polyimide coated SMF. These were sealed (using a feedthrough) inside high-pressure stainless-steel tubing (2 mm internal diameter) filled will oil. The pressure was increased up to 200 bar using a DHI PPCH controller. The results show that the transmission peak appears to start splitting at 150 bar and two peaks become visible at 200 bar. At 200 bar the peak separation is approximately 240 pm, leading to an estimated sensitivity of 1.2 pm/bar.

The proposed fabrication technique can potentially be applied to many different fibers. Sapphire optical fiber is particularly attractive as it withstand temperatures up to 2000°C and high radiation. Recently, a single-mode sapphire optical fiber has been demonstrated using femtosecond laser fabrication [11] and sapphire can be etched with very high selectivity using KOH [12]. The new fabrication technique therefore opens up the possibility of optical fiber pressure sensing in ultra-extreme environments.

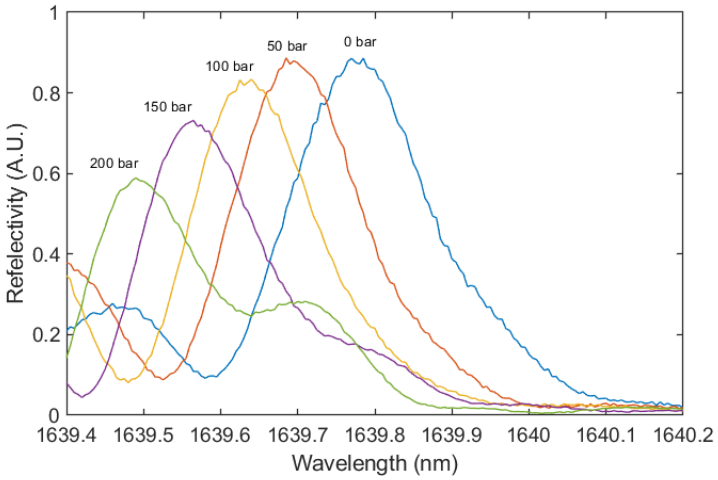


Fig. 5. Preliminary pressure test result of the sector holes with elliptical micro-holes sample.

4. Conclusions

We demonstrated a new method of pressure sensor fabrication using femtosecond laser writing and selective etching, allowing high sensitivity without incurring high splice losses. Simulations show large pressure sensitivities of up to 3.2 pm/bar are possible in 250 μm diameter fiber. We fabricated 3D pressure sensors in both standard single-mode fiber and a large diameter fiber. Initial oil-based pressure testing showed a pressure sensitivity of 1.2 pm/bar. The fabrication technique has the potential to be used in a wide range of high performance fibers, including sapphire fiber for use in ultra-extreme environments.

References

1. L. Albero Blanquer, F. Marchini, J. R. Seitz, N. Daher, F. Bétermier, J. Huang, C. Gervillié, and J.-M. Tarascon, "Optical sensors for operando stress monitoring in lithium-based batteries containing solid-state or liquid electrolytes," *Nature communications*, vol. 13, no. 1, pp. 1–14, 2022.
2. Y. Zhao, Y. Zhu, M. Yuan, J. Wang, and S. Zhu, "A laser-based fiber bragg grating ultrasonic sensing system for structural health monitoring," *IEEE Photonics Technology Letters*, vol. 28, no. 22, pp. 2573–2576, 2016.
3. T. Kao and H. Taylor, "High-sensitivity intrinsic fiber-optic fabry–perot pressure sensor," *Optics letters*, vol. 21, no. 8, pp. 615–617, 1996.
4. C. M. Jewart, Q. Wang, J. Canning, D. Grobnic, S. J. Mihailov, and K. P. Chen, "Ultrafast femtosecond-laser-induced fiber bragg gratings in air-hole microstructured fibers for high-temperature pressure sensing," *Optics letters*, vol. 35, no. 9, pp. 1443–1445, 2010.
5. T. Chen, Q. Wang, R. Chen, B. Zhang, C. Jewart, K. P. Chen, M. Maklad, and P. R. Swinehart, "Distributed high-temperature pressure sensing using air-hole microstructural fibers," *Optics letters*, vol. 37, no. 6, pp. 1064–1066, 2012.
6. T. Chen, R. Chen, C. Jewart, B. Zhang, J. Canning, K. Cook, and K. P. Chen, "Thermally regenerated fiber bragg gratings in twin-air-hole microstructured fibers for high temperature pressure sensing," in *Fiber Optic Sensors and Applications VIII*, vol. 8028, pp. 32–39, SPIE, 2011.
7. J.-Y. Huang, J. Van Roosbroeck, J. Vlekken, A. B. Martinez, T. Geernaert, F. Berghmans, B. Van Hoe, E. Lindner, and C. Caucheteur, "Fbgs written in specialty fiber for high pressure/high temperature measurement," *Optics express*, vol. 25, no. 15, pp. 17936–17947, 2017.
8. D. Goldstein, *Polarized Light*. CRC Press, 2017.
9. S. Kiyama, S. Matsuo, S. Hashimoto, and Y. Morihira, "Examination of etching agent and etching mechanism on femotosecond laser microfabrication of channels inside vitreous silica substrates," *The Journal of Physical Chemistry C*, vol. 113, no. 27, pp. 11560–11566, 2009.
10. L. Wong, T. Suratwala, M. Feit, P. Miller, and R. Steele, "The effect of hf/nh4f etching on the morphology of surface fractures on fused silica," *Journal of Non-Crystalline Solids*, vol. 355, no. 13, pp. 797–810, 2009.
11. M. Wang, P. S. Salter, F. P. Payne, A. Shipley, S. M. Morris, M. J. Booth, and J. J. Fells, "Single-mode sapphire fiber bragg grating," *Optics Express*, vol. 30, no. 9, pp. 15482–15494, 2022.
12. M. Kaiser, M. Kumkar, R. Leute, J. Schmauch, R. Priester, J. Kleiner, M. Jenne, D. Flamm, and F. Zimmermann, "Selective etching of ultrafast laser modified sapphire," in *Laser Applications in Microelectronic and Optoelectronic Manufacturing (LAMOM) XXIV*, vol. 10905, pp. 19–30, SPIE, 2019.